Optical interconnection of core and metro networks [Invited]

A. D. Ellis,[1,*] D. Cotter,[1] S. Ibrahim,[1] R. Weerasuriya,[1] C. W. Chow,[1,2] J. Leuthold,[3] W. Freude,[3] S. Sygletos,[3] P. Vorreau,[3] R. Bonk,[3] D. Hillerkuss,[1,3] I. Tomkos,[4] A. Tzanakaki,[4] C. Kouloumentas,[4] D. J. Richardson,[5] P. Petropoulos,[5] F. Parmigiani,[5] G. Zarris,[6] and D. Simeonidou[6]

[1]*Photonic Systems Group, Department of Physics, University College Cork, Cork, Ireland*
[2]*Currently with Department of Photonics, National Chiao Tung University, Hsinchu, Taiwan*
[3]*Institute of High-Frequency and Quantum Electronics, University of Karlsruhe, 76131 Karlsruhe, Germany*
[4]*Athens Information Technology, Athens, Greece*
[5]*Optoelectronics Research Centre, University of Southampton, United Kingdom*
[6]*Photonic Networks Research Laboratory, CES, University of Essex, Colchester CO4 3SQ, UK*
[*]*Corresponding author: andrew.ellis@tyndall.ie*

Received July 23, 2008; revised September 16, 2008; accepted September 21, 2008; published October 22, 2008 (Doc. ID 99278)

A network concept is introduced that exploits transparent optical grooming of traffic between an access network and a metro core ring network. This network is enabled by an optical router that allows bufferless aggregation of metro network traffic into higher-capacity data streams for core network transmission. A key functionality of the router is WDM to time-division multiplexing (TDM) transmultiplexing. © 2008 Optical Society of America

OCIS codes: 060.2330, 060.4250, 060.4510.

1. Introduction

Optical transparency is widely recognized to play a central role in next-generation optical networks and to offer significant networking advancements in terms of performance and cost [1]. The scalability of optical technology and the elimination of expensive optical-electrical-optical (OEO) equipment is expected to significantly reduce the capital costs, whereas operational cost savings are expected to result from reduced power requirements and the flexibility of transparent service provisioning. The first steps toward this goal were point-to-point links routed via optical add–drop multiplexers (OADMs) at intermediate nodes, and increasingly the trend is toward so-called islands of transparency, with the eventual aim of fully meshed transparent optical networks with reconfigurable optical cross connects (OXCs) [2]. These islands of transparency allow optical connectivity with variable bit rates independent of other islands. Initial commercial activity consists of several regional systems that are interconnected via reconfigurable OADMS (ROADMs) and OXCs to provide transparency extending over a substantial portion of a continental area [3], typically corresponding to a single service provider.

These initial activities have been almost exclusively focused on developing the core part of transparent networks [4–6], in complete isolation from the metro and access segment [7,8]. Currently, the gateway routers between these segments are based on optoelectronic (OE) conversion and buffer stores. Any proposed solution for these gateway routers must be competitive in terms of both performance and cost, while also providing additional protocol-specific management functionality. Such routers should thus be able not only to perform the traditional switching and routing and protection functionalities but also to offer mechanisms for traffic aggregation and grooming, i.e., subwavelength switching granularity, for traffic flowing between the segments and also between carriers within either segment.

In this paper, we summarize our recent publications in order to discuss an implementation of a gateway router with sufficient grooming functionality to enable full interoperability between burst-switched lower-bit-rate access and metro networks and a higher-bit-rate core-ring network [9,10]. A typical network scenario in which the

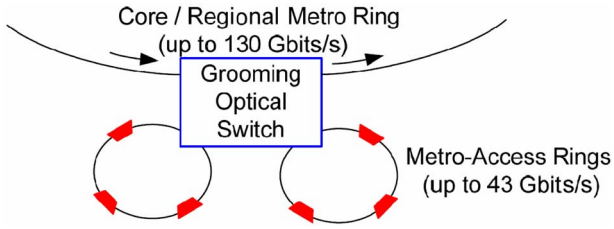

Fig. 1. Network scenario: several metro and access rings are interconnected to a core or regional metro ring network [10].

router might be deployed is depicted in Fig. 1. This shows two access networks carrying 10 to 40 Gbits/s data bursts that are interconnected with each other but may also be aggregated to higher-speed (130 Gbits/s) data bursts on the core ring. Similarly 10 or 40 Gbits/s data bursts may be extracted from the regional metro ring and either dropped to one of the access rings or switched to another time slot or carrier within the core ring. It should be noted that to maximize network efficiency, all reconfiguration operations should take place between bursts (i.e., in the guard band), and any routing decisions should take place within a single burst, assuming pipelined operation.

2. Implementation of the Gateway Router

The architecture of the gateway router is depicted in Fig. 2. The router interconnects two access rings, each carrying one or more 43 Gbits/s WDM channels, with a metro core ring with two or more 130 Gbits/s channels. The router works as follows: traffic from any of the access rings is switched by means of an optical cross-connect switch onto either access ring or via the add path onto the core ring. Asynchronous data bursts are presented to the input of the WDM-to-optical-TDM (OTDM) unit, where each burst is retimed to a local clock and its wavelength is converted to a signal comprising suitably short high-speed pulses of the OTDM channel at a desired wavelength. The retimed data bursts are then time interleaved to form the OTDM signal and injected into the core ring using a wavelength-selective switch (WSS). In this work, the retiming is performed using an asynchronous digital optical regenerator (ADORE) [11–14], with one such unit available for each tributary to avoid wavelength blocking, with time-slot assignment determined by the selection of the appropriate ADORE using the optical cross connect. On exiting the core network, via the WSS, the OTDM tributaries are simultaneously extracted using a multiwavelength probe signal applied to a single nonlinear optical gate, the time-slot-to-wavelength mapping being

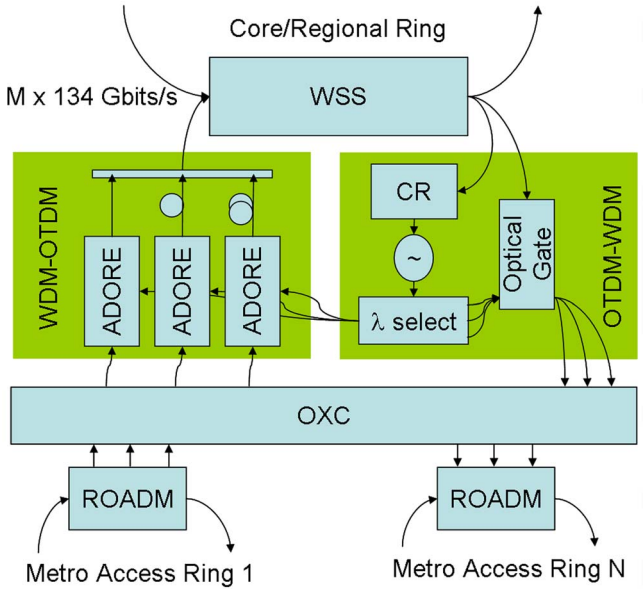

Fig. 2. Gateway router configuration.

determined by the arrangement of the probe wavelengths. Each demultiplexed OTDM tributary then passes to the OXC, where it is mapped onto either of the access rings or back onto the core ring via the ADORE units. By selecting the appropriate ADORE path, time-slot interchange may also be performed for any looped-back tributaries, as required. The node clock signal used to drive the ADORE circuits is extracted from a dropped OTDM signal or provided locally if no core traffic is dropped.

3. WDM-to-OTDM Conversion

OTDM multiplexing of several lower-bit-rate channels requires shortening the pulse widths of the tributaries, mapping all the tributaries onto a common wavelength, and introducing precise relative timing delays between the signals so that pulses from neighboring channels do not overlap after optical multiplexing. Although many techniques have been proposed for pulse generation, wavelength conversion, and multiplexing [15–17], little attention has been paid to the optical retiming of incoming signals necessary to allow bit-level alignment of the OTDM tributaries. This is of particular importance since incoming low-speed data signals from multiple sources may have slightly different clock frequencies [up to 4.6 parts per billion for synchronous digital hierarchy (SDH) signals in holdover mode [18]] and suffer from inevitable environmentally induced changes in propagation delays. Although signals may be retimed using distributed phase-locked loops [19] and all-optical delays [20], such techniques restrict the total circumference of the metro ring due to a combination of phase noise, maximum delay tunability, and fly-back. For a burst-switched network, however, an incoming data burst may be simultaneously sampled at multiple clock phases [21], and subsequently, the optimum clock phase is selected for onward processing. Such a scheme may be developed for use in optical systems [11–13] and may also provide partial regeneration of the incoming signal. One promising implementation is known as the ADORE. The functional diagram of the ADORE [11] scheme is shown in Fig. 3. In the ADORE, an incoming data burst is simultaneously sampled at N different clock phases—four in this example—each delayed by T/N bit-slot durations with respect to its neighbor, where T is the bit period. To achieve this, optical clock pulses at the gateway router clock frequency (f_L) probe each of the N gates with successive delays of $1/(Nf_L)$. Each bit of the input data burst (at a frequency f_R) simultaneously modulates all four gates with a switching window of at least $1/N$ of the bit period, such that the switching window of at least one gate overlaps with one of the copies of the local clock pulse irrespective of the relative phase of the incoming data. For free-running clock sources within permitted limits [18], it can be shown that the relative phase difference varies by an insignificant amount for bursts of up to 4,000 bytes [11]. By selecting the optimum sampling, clock phase signal retiming is achieved; furthermore, if the phase delays before the optical gates are reversed following modulation, all possible clock phase paths are of identical total length. Thus the output signal will be at a known frequency and phase, irrespective of the incoming phase difference. The data burst is thus retimed, and amplitude regeneration is achieved through the selection of an optical gate with an appropriate nonlinear transfer function.

Since the optical data burst is unipolar, the optimum channel may be determined following gating by selecting the path with the highest mean power. However, the optimum channel may also be determined by mixing the local clock with the incoming data signal electronically, so that the mixer output voltage is proportional to the

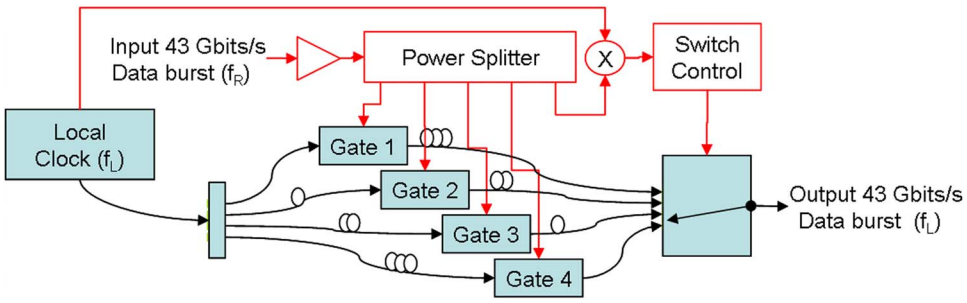

Fig. 3. Functional diagram of the ADORE.

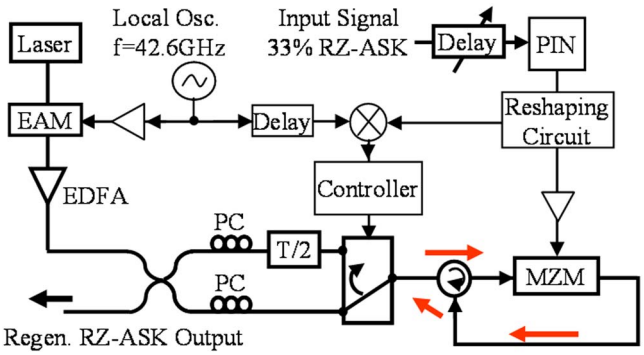

Fig. 4. Experimental configuration of the ADORE [13].

cosine of the phase difference between the input data signal and the local clock [13]. In this case, switching may be performed before modulation, ensuring that only the appropriate clock phase is modulated, as demonstrated in the experiment whose setup is shown in Fig. 4(a). dual-gate ADORE was based on a single optical gate configured to optimally modulate one of two half-bit delayed probe pulses preselected by a 2×1 optical switch. To generate local optical clock pulses, an electroabsorption modulator (EAM) was driven by a locally generated 42.6 GHz clock signal to generate ~5 ps probe pulses at the wavelength of a local cw laser source at 1549.7 nm. Then an erbium-doped fiber amplifier (EDFA) was used to amplify the optical pulses before being split by a 3 dB coupler and passed through two optical paths containing polarization controllers and a differential optical delay of $T/2$, equivalent to ~11.72 ps. The two probe pulses were then passed to a 2×1 optical switch that was automatically controlled by a circuit that selected the probe pulse giving the best sampling point. To demonstrate the operation of the ADORE, a 42.6 Gbits/s 33% return-to-zero amplitude-shift-keying (RZ-ASK) data signal with a pseudorandom binary sequence (PRBS) length of 2^7-1 and a back-to-back sensitivity of ~−32.2 dBm at a wavelength of 1558.7 nm was generated using an external-cavity laser and two lithium niobate ($LiNbO_3$) Mach–Zehnder modulators (MZMs). This signal passed through a variable optical delay line and was amplified to a total power of +4.5 dBm before entering the ADORE circuit of Fig. 4. The RZ-ASK signal was detected using a high-speed p-i-n photodiode, then reshaped to a non-return-to-zero (NRZ) ASK signal by use of a high-speed comparator. This reshaping function guaranteed a wider switching window for the ADORE, which in turn ensured correct gating for a wide range of relative phases. The signal was then electrically amplified and applied to the electrodes of a $LiNbO_3$ MZM biased at the quadrature point. Depending on the position of the 2×1 switch, the MZM modulated one of the probe pulses resulting in a regenerated RZ-ASK signal with the same wavelength and pulse width as the probe pulses. The regenerated RZ-ASK signal was then returned to the switch through a circulator and passed through the same path of the probe signal resulting in a total relative delay of either 0 or T, depending on which probe signal was used. The retimed signal was thus bit aligned for subsequent OTDM multiplexing, although the timing of the data burst at the output of the ADORE, relative to the input, may vary stochastically by one bit period with negligible consequence on network throughput.

The performance of the ADORE was evaluated by measuring the bit error rate (BER) curves of the regenerated signal for different delay phases between the incoming data signal and the local clock as shown in Fig. 5. The automatic channel selection control of the switch ensured that error-free performance was achieved for the whole range of delay phases. The receiver sensitivity penalty was measured to vary between 1 and 3 dB. Also shown in Fig. 5 are the eye diagrams of the regenerated RZ-ASK signal for both worst-case delay (top) and best-case delay (bottom) for the regenerated RZ-ASK signal. As may be seen, the majority of the receiver sensitivity penalty may be attributed to a slight degradation in the extinction ratio corresponding to small-level signal leaking through from adjacent bit slots for the worst-case relative phase.

If the locally generated probe pulses are replaced with 2 ps pulses from a mode-locked semiconductor laser, it is possible to complete the WDM-to-OTDM converter of Fig. 2 by combining the outputs of multiple optical gates. The resultant eye diagram is shown in Fig. 6, where the full MZM-based ADORE with a random phase is OTDM

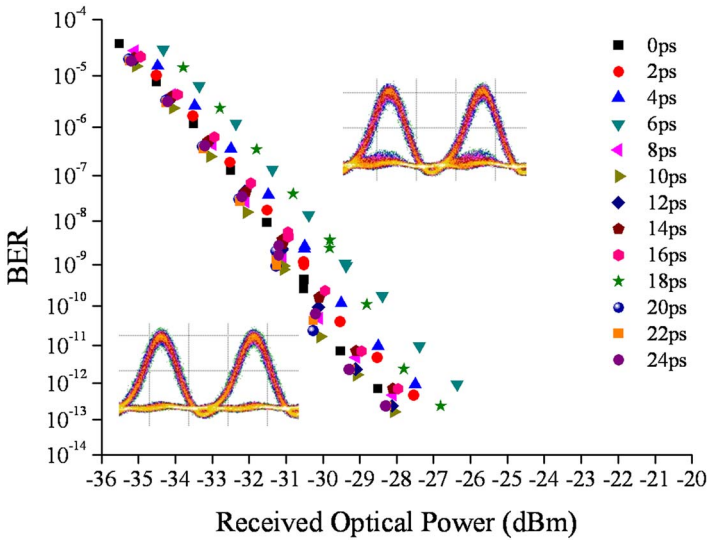

Fig. 5. Bit error rate measurements of a MZM-based ADORE circuit.

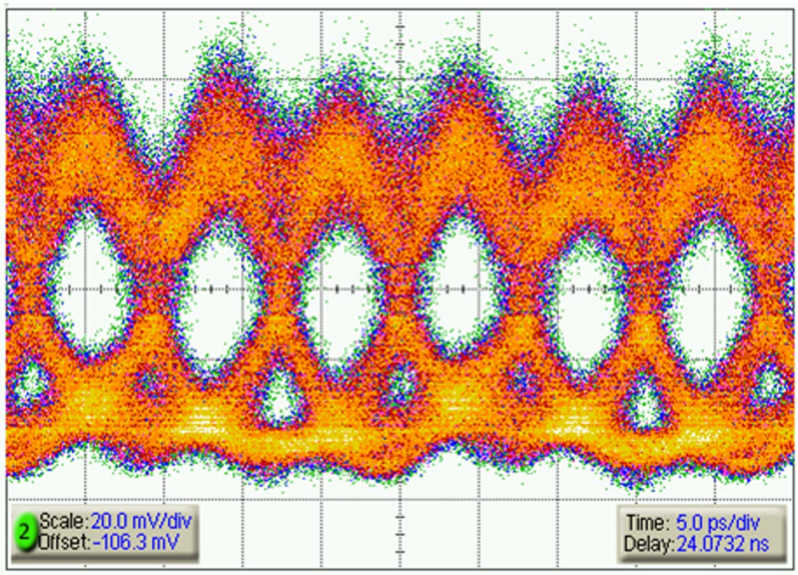

Fig. 6. OTDM multiplexing using the ADORE.

multiplexed with the outputs of two semiconductor optical amplifier interferometer-based optical wavelength converters [22] operated at the optimum phase delay.

4. OTDM-to-WDM Conversion

The gateway router is completed by demultiplexing selected OTDM channels back to an appropriate number of WDM channels, which are input to the router cross connect to enable time-slot interchange, looping back, or routing to either access ring [10,23]. A schematic diagram of the OTDM-to-WDM converter, configured for 128.1 Gbits/s TDM to three 42.6 Gbits/s WDM demultiplexing, is shown in Fig. 7. Three 42.6 GHz clocks ($\lambda_{1,2,3}$) are temporally aligned to different time slots of the TDM signal and are launched into the input port of a nonlinear optical loop mirror (NOLM), which is used as the nonlinear optical gate shown in Fig. 2. If a TDM pulse (at wavelength λ_0) is present (ones), a nonlinear phase shift is induced onto the copropagating clock pulse that is temporarily aligned with the respective pulse. The induced phase shift will lead to a constructive interference of the copropagating and counterpropagating clock pulse into the output. This allows coded information to be effectively transferred from specific time slots at one wavelength to different wavelengths. However, the required

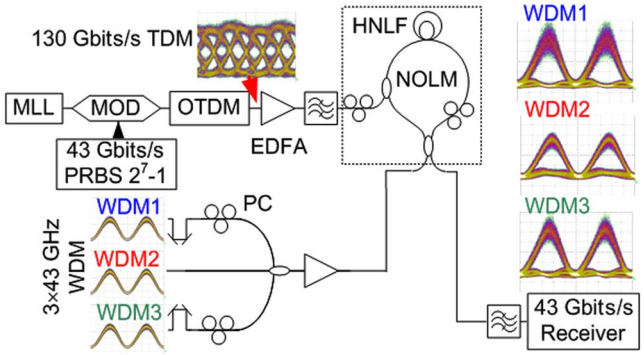

Fig. 7. Schematic diagram of OTDM-to-WDM conversion [23].

p phase shift also induces a significant spectral broadening on the probe channel, proportional to the phase shift and the spectral width of the 128.1 Gbits/s drive signal. In this example, the 0.8 nm probe signals are each broadened to approximately 2 nm. For effective multiwavelength operation of the NOLM, it is necessary to ensure that efficient cross-phase modulation occurs with low walk-off and uniform switching efficiency with good jitter tolerance, operable across the whole bandwidth of the clock signals. To achieve this, accurate control of the dispersion and dispersion slope of the fiber is needed, while minimizing the resultant spectral overlap of the signals. Following extensive numerical simulations, a highly nonlinear fiber (HNLF) fabricated by Furukawa Electric Co., Tokyo, Japan, was selected for the loop with a length of 310 m, a dispersion of 0.31 ps/nm/km, a dispersion slope of 0.0031 ps/nm^2/km, a nonlinear coefficient of 22/W/km, and a loss of 1.21 dB/km. These fiber parameters result in a maximum walk-off time between the OTDM drive signal and the various WDM clock signals of only 1.8 ps, while minimizing the unwanted spectral broadening.

The experiment depicted in Fig. 7 shows how a 128.1 Gbits/s TDM channel operated at $\lambda_0 = 1539.4$ nm and generated with a mode-locked laser (MLL) giving 2.5 ps pulses is mapped onto three ~6 ps clock signals at wavelengths of $\lambda_1 = 1547.8$ nm, $\lambda_2 = 1552.5$ nm, and $\lambda_3 = 1557.4$ nm. The total power of the three clock signals in the loop was ~20 dBm, and the TDM signal was ~23 dBm, before entering the NOLM via a 3 dB coupler. The WDM signals switched by the NOLM were then separated by a WDM demultiplexer filter and individually assessed using a preamplified receiver, which consisted of a variable attenuator, an EDFA, an ~1 nm filter, and a 40 GHz receiver. Figure 8 shows the spectral traces at the output port of the NOLM, along with bit error rate measurements for different combinations of probe channels present.

Receiver sensitivity penalties between 0 and 6 dB were observed due to the aforementioned spectral cross talk, together with unequalized clock pulse amplitudes.

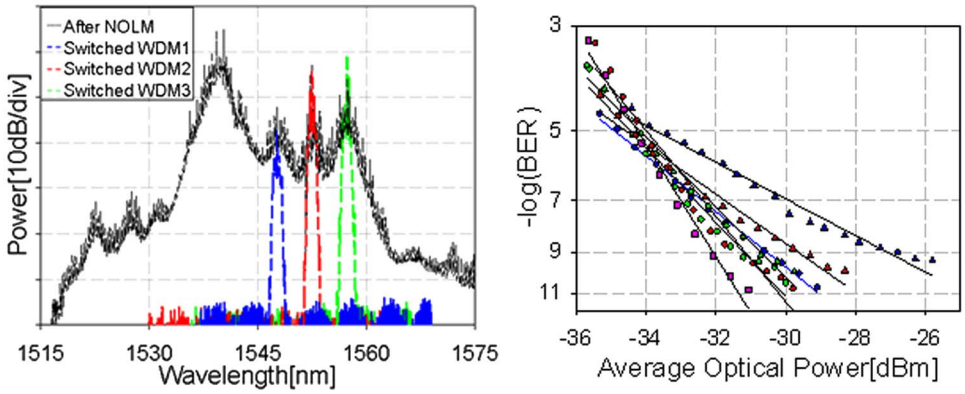

Fig. 8. Left, spectral traces of the demultiplexed switched signal before (solid curve) and after (dashed curves) the WDM filter. Right, BER measurements of each WDM channel when the other WDM channels are absent (circles) and present (triangles), respectively. The 40 Gbits/s back-to-back measurements are also shown (rectangles) [23].

5. Conclusions

In this work we have described the operating principle of an optical gateway router that enables optical interconnection of network segments operating at different line rates, while avoiding the need for electronic buffer stores and multiple transponders (one for each tributary channel). We have experimentally demonstrated the two key building blocks of this gateway router, namely, the asynchronous digital optical regenerator, allowing clock frequency adaptation and enabling multiplexing to higher data rates, and an optimized nonlinear optical loop mirror, allowing the distribution of high-data-rate signals to multiple WDM channels.

Acknowledgments

This work was supported by the European project TRIUMPH (grant IST-027638 STP), by the Center for Functional Nanostructures (CFN) of the Deutsche Forschungsgemeinschaft (DFG) within Project A4.4 and by Science Foundation Ireland (grant 06/IN/I969), and the authors thank the Furukawa Electric Company, Japan, for the loan of the HNLF.

References

1. S. Sygletos, I. Tomkos, and J. Leuthold, "Technological challenges on the road toward transparent networking," J. Opt. Netw. **7**, 321–350 (2008).
2. A. A. M. Saleh, "All-optical networking in metro, regional and backbone networks," in *IEEE/LEOS Summer Topical Meeting on All-Optical Networks* (IEEE, 2002), Mg3–15.
3. D. Fishman, D. L. Correa, E. H. Goode, T. L. Downs, A. Y. Ho, A. Hale, P. Hofmann, B. Basch, and S. Gringeri, "The rollout of optical networking: LambdaXtreme national network deployment," Bell Lab. Tech. J. **11**, 55–63 (2006).
4. S. J. B. Yoo, "Optical packet and burst switching technologies for the future photonic internet," J. Lightwave Technol. **24**, 4468–4492 (2006).
5. D. J. Blumenthal, B. E. Olsson, G. Rossi, T. E. Dimmick, L. Rau, M. Masanovic, O. Lavrova, R. Doshi, O. Jerphagnon, J. E. Bowers, V. Kaman, L. A. Coldren, and J. Barton, "All-optical label swapping networks and technologies," J. Lightwave Technol. **18**, 2058–2075 (2000).
6. A. Al Amin, K. Shimizu, M. Takenaka, T. Tanemura, R. Inohara, K. Nishimura, Y. Horiuchi, M. Usami, Y. Takita, Y. Kai, Y. Aoki, H. Onaka, Y. Miyazaki, T. Miyahara, T. Hatta, K. Motoshima, T. Kagimoto, T. Kurobe, A. Kasukawa, H. Arimoto, S. Tsuji, H. Uetsuka, and Y. Nakano, "40/10 Gbps bit-rate transparent burst switching and contention resolving wavelength conversion in an optical router prototype," in *Proceedings of the European Conference on Optical Communication* (SEE, 2006), paper PDP.Th.4.1.6.
7. C. W. Chow, G. Talli, A. D. Ellis, and P. D. Townsend, "Rayleigh noise mitigation in DWDM LR-PONs using carrier suppressed subcarrier-amplitude modulated phase shift keying," Opt. Express **16**, 1860–1866 (2008).
8. D. Shea, A. D. Ellis, D. Payne, R. Davey, and J. Mitchell, "10 Gbit/s PON with 100 km reach and ×1024 split," in *Proceedings of the European Conference on Optical Communication* (AEI, 2003), paper We.P.147.
9. I. Tomkos, A. Tzanakaki, J. Leuthold, A. D. Ellis, D. Bimberg, P. Petropoulos, D. Simeonidou, S. Tsadka, and P. Monteiro, "Transparent ring interconnection using multi-wavelength processing switches," in *International Conference on Transparent Optical Networks* (IEEE, 2006), paper Mo.B.1.5.
10. J. Leuthold, W. Freude, S. Sygletos, P. Vorreau, R. Bonk, D. Hillerkuss, I. Tomkos, A. Tzanakaki, C. Kouloumentas, D. J. Richardson, P. Petropoulos, F. Parmigiani, A. Ellis, D. Cotter, S. Ibrahim, and R. Weerasuriya, "An all-optical grooming switch to interconnect access and metro ring networks," in *10th American International Conference on Transparent Optical Networks* (IEEE, 2008), invited paper We.C3.4.
11. D. Cotter, A. D. Ellis, "Asynchronous digital optical regeneration and networks," J. Lightwave Technol. **16**, 2068–2080 (1998).
12. C. W. Chow, A. D. Ellis, and D. Cotter, "Asynchronous digital optical regenerator for 4 ×40 Gbit/s WDM to 160 Gbit/s OTDM conversion," Opt. Express **15**, 8507–8512 (2007).
13. S. K. Ibrahim, R. Weerasuriya, D. Hillerkuss, G. Zarris, D. Simeonidou, J. Leuthold, D. Cotter, and A. Ellis, "Experimental demonstration of 42.6 Gbit/s asynchronous digital optical regenerators," in *10th Anniversary International Conference on Transparent Optical Networks* (IEEE, 2008), invited paper We.C3.3.
14. S. K. Ibrahim, D. Hillerkuss, R. Weerasuriya, G. Zarris, D. Simeonidou, J. Leuthold, and A. D. Ellis, "Novel 42.65 Gbit/s dual gate asynchronous digital optical regenerator using a single MZM," in *Proceedings of the European Conference on Optical Communication* (IEEE, 2008), paper Tu4.D.3.
15. K. Uchiyama and T. Morioka, "All-optical signal processing for 160 Gbit/s/channel OTDM/WDM systems," in *Optical Fiber Communication Conference*, 2001 OSA Technical Digest Series (Optical Society of America, 2001), paper ThH2.
16. M. Hayashi, H. Tanaka, K. Ohara, T. Otani, and M. Suzuki, "OTDM transmitter using

WDM-TDM conversion with an electroabsorption wavelength converter," J. Lightwave Technol. **20**, 236–242 (2002).
17. B.-E. Olsson and D. J. Blumenthal, "WDM to OTDM multiplexing using an ultrafast all-optical wavelength converter," IEEE Photon. Technol. Lett. **13**, 1005–1007 (2001).
18. M. Sexton and A. Reid, *Transmission Networking: SONET and the SDH* (Artech House, 1992).
19. A. D. Ellis, T. Widdowson, I. D. Phillips, and W. A. Pender, "High speed optical TDM networks employing electro-optic modulators," IEICE Trans. Electron. **E81-C**, 1301–1308 (1998).
20. J. Ren, N. Alic, E. Myslivets, R. E. Saperstein, C. J. McKinstrie, R. M. Jopson, A. H. Gnauck, P. A. Andrekson, and S. Radic, "12.47 ns continuously-tunable two-pump parametric delay," in *Proceedings of the European Conference on Optical Communication* (SEE, 2006), postdeadline paper Th4.4.3.
21. M. Banu and A. E. Dunlop, "Clock recovery circuits with instantaneous locking," Electron. Lett. **28**, 2127–2130 (1992).
22. G. Maxwell, "Low-cost hybrid photonic integrated circuits using passive alignment techniques," in *19th Annual Meeting of the IEEE Lasers and Electro-Optics Society* (IEEE, 2006), pp. 98–99.
23. P. Vorreau, F. Parmigiani, K. Mukasa, M. Ibsen, P. Petropoulos, D. J. Richardson, A. Ellis, W. Freude, and J. Leuthold, "TDM-to-WDM conversion from 130 Gbit/s to 3×43 Gbit/s using XPM in a NOLM switch," in *10th Anniversary International Conference on Transparent Optical Networks* (IEEE, 2008), postdeadline paper Th.PD2.